Open Economies Review
https://doi.org/10.1007/s11079-025-09807-7

ORIGINAL RESEARCH

Do Changes in the Real Exchange Rate Affect the Trade Balance? Evidence from European Countries

Jesus Felipe[1] · **José A. Pérez-Montiel**[2] · **Oguzhan Ozcelebi**[3]

Accepted: 5 May 2025

Abstract

We use time and frequency domain causality tests to study whether unit-labor-costs-based real exchange rate depreciations/appreciations caused improvements/deteriorations in the trade balances of ten Eurozone economies, and thus contributed to closing trade imbalances, during 1995–2019. The methods we use deal with the inherent nonlinearity and structural shifts in the time series. They also consider asymmetry and regime changes. The non-parametric approach avoids the possible bias associated to the identification strategy. Test results indicate that, for most countries, exchange rate movements do not cause the trade balance dynamics. Hence, policy strategies solely focused on exchange rate adjustments may not be enough to overcome trade imbalances.

Keywords Exchange rate · Trade balance · Europe

JEL Classifications C14 · C32 · F16 · J31

We are grateful to the participants at research seminars at Sant'Anna Scuola Universitaria Superiore Pisa and at the International Astril Conference. The usual disclaimer applies.

✉ José A. Pérez-Montiel
jose.perez@uib.es

Jesus Felipe
jesus.felipe@dlsu.edu.ph

Oguzhan Ozcelebi
ogozc@istanbul.edu.tr

[1] De La Salle University, Manila, Philippines

[2] University of the Balearic Islands, Palma, Spain

[3] Istanbul University, Istanbul, Turkey

Published online: 17 June 2025

1 Introduction

Have real exchange rate shifts contributed to closing (increasing) trade imbalances in the European Union? A widely accepted explanation of the increasing trade imbalances in the Eurozone before 2008 focuses on the functioning of the Economic and Monetary Union (EMU). This explanation argues that the creation of the EMU reduced the risk premia of the European peripheral economies, which led to a consumption and investment boom and, thus, to higher inflation and a loss of competitiveness (via higher unit labor costs) in these countries (Allsop and Vines 2010; Krugman 2012; Belke and Dreger 2013; El-Shagi et al. 2016).

Following the global financial crisis of 2008–09 (GFC hereafter), "peripheral" Euro countries (Greece, Ireland, Italy, Spain) were asked (until the Covid-19 crisis) to lower their real wage rates and to increase productivity to reduce their unit labor costs. This was referred to as the *internal depreciation* mechanism.[1] "Core" Euro countries (Finland, France, Germany, Luxemburg, Netherlands, Belgium), on the other hand, were asked to increase their real wage rates and implement policies to increase domestic demand, which would lead to an increase in their unit labor costs. The European Commission supported this strategy to overcome the GFC: "internal devaluation is a set of policies aimed at reducing domestic prices (to regain competitiveness) either by affecting relative export–import prices or by lowering domestic production costs and thus by yielding a real exchange rate depreciation" (European Commission 2011: 22). This economic policy recommendation rests on the idea that real exchange rate adjustments affect the trade balance of the Eurozone economies.

The years after the GFC saw a marked improvement in the trade balances of the Mediterranean economies (Fig. 1). According to Hein et al. (2021) and Kohler & Stockhammer (2022), wage restraint and austerity policies contributed to improving the trade balance through the collapse of domestic demand and imports. Figure 1 shows that net exports of Europe's peripheral countries gradually deteriorated right after the start of the second phase of the monetary integration in 1994. Core countries, on the other hand, maintained or increased their trade surpluses. After the 2008–09 crisis, however, the trade deficits of the peripheral countries declined, while the surpluses of some core countries became smaller. This may suggest that internal depreciations led to reductions in the trade imbalances of the European Union.

This paper explores whether internal depreciations/appreciations corrected trade imbalances in the eurozone during 1995–2019. We shed light on this question by analyzing the dynamic causal relationship between the real effective exchange rate based on unit labor costs (q_t) and the trade balance (tb_t). More precisely, we study if negative (positive) changes in q_t caused negative (positive) changes in tb_t in ten Euro Zone economies.

The relationship between q_t and tb_t has been studied empirically within the approach of Goldstein and Khan (1985). This approach defines the domestic trade

[1] Given that the members of the Eurozone cannot modify the nominal exchange rates, real exchange rate changes have to result from changes in domestic prices or in production costs.

balance (tb) as a function of domestic and foreign real income (Y and Y^*, respectively) and the real exchange rate (q):

$$tb = f(Y, Y^*, q). \tag{1}$$

where $\frac{\partial tb}{\partial Y} > 0$, $\frac{\partial tb}{\partial Y^*} < 0$, $\frac{\partial tb}{\partial q} \gtrless 0$, with tb defined as the ratio imports to exports. The sign of $\frac{\partial tb}{\partial q}$ is indeterminate and depends on the price elasticities of exports (ψ) and imports (η). The Marshall-Lerner condition states that the trade balance will improve if the absolute value of the sum of the price elasticities of exports and imports is greater than one, that is $(\frac{\partial tb}{\partial q}\frac{q}{tb}) > 0$ if $|\psi + \eta| > 1$. Following the seminal contribution by Rose and Yellen (1989), a strand of the empirical literature obtains the elasticity of the trade balance with respect to the real exchange rate by directly estimating (1) as:

$$lntb_t = \alpha + \beta_1 lnY_t^* + \beta_2 lnY_t + \beta_3 lnq_t \tag{2}$$

If $\beta_3 > 0$ and statistically significant, it is concluded that a depreciation (appreciation) improves (worsens) the trade balance in the long run. Some applications allow for a dynamic response of the different explanatory variables, so that the short-term elasticity of the exchange rate can be smaller than the long-term elasticity, thereby producing a J-curve effect (Magee 1973).

The J-curve hypothesis has been tested through different econometric methods on many occasions and in different settings. In general, results are mixed and, thus, there is no consensus in the empirical literature on the J-curve theory. In the case of the Euro zone, results are also inconclusive (see Bahmani et al. (2013) and Bahmani-Oskooee and Nouira (2021a)). Most studies assume that changes in real exchange rates have symmetric effects on the trade balance; however, Bahmani-Oskooee & Fariditavana (2016) and Bahmani-Oskooee & Nouira (2021b) have argued and

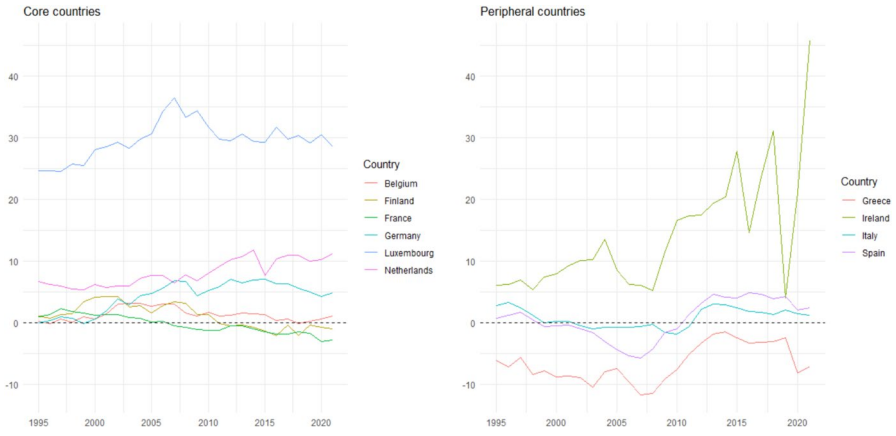

Fig. 1 Net exports as percentage of GDP (1995–2019). Source: Authors based on Eurostat data. Note: vertical axis is "Net exports as % of GDP", calculated as: ((exports-imports)/GDP)*100

shown that exchange rate changes are more likely to affect asymmetrically the trade balance. Indeed, if an x% depreciation improves the trade balance by y%, an x% appreciation might not necessarily worsen the trade balance by y% if traders' expectations change when a currency appreciates compared to when it depreciates. The relationship between q and tb can also be nonlinear due to macroeconomic instability, structural breaks, etc.

After the contribution of Bahmani-Oskooee & Fariditavana (2016), several studies have tested the J-curve hypothesis by means of nonlinear regression techniques (see Karamelikli 2016; Nusair 2016; Ivanovski et al. 2020; Bahmani-Oskooee & Karamelikli 2021a, 2021b; Iqbal et al. 2021; Upadhyaya et al. 2022; Mwito et al. 2021). Our paper pushes the debate further by applying a framework that captures the nonlinear, time-varying, and the regime-dependent nature of the nexus between the exchange rate and the trade balance. First, we apply a battery of non-parametric causality tests in the time domain. The tests are the parametric causality-in-quantile test of Troster (2018), the nonparametric causality-in-quantile test of Balcilar et al. (2017), and the rolling-window Granger-causality test of Hacker and Hatemi-J (2012). Additionally, we test if the variables are correlated in the frequency domain by mans of the wavelet coherence (WC) approach and the Wavelet Quantile Correlation (WQC) technique of Li et al. (2015). The main advantages of the causality tests that we apply is that they overcome many of the shortcomings of the traditional Granger causality tests used in the exchange rate-trade balance literature (Bahmani-Oskooee and Nouira 2021b). They deal with the inherent nonlinearity and structural shifts in the time series, consider asymmetry and regime changes, and avoid the possible bias associated to the identification strategy. Thus, our paper differs from other studies in that our methodology more accurately accounts for the complexity of the underlying relationship between the exchange rate and the trade balance.

The remainder of the paper is structured as follows. Section 2 describes the variables and the empirical approach. Section 3 describes our econometric methodology. Section 4 discusses the empirical results. Finally, Sect. 5 concludes. The Appendix provides details of the tests we use.

2 Data and empirical approach

In this paper, we focus on the relationship between tb_t and q_t in ten European economies for the period 1995:Q1-2019:Q4. These economies are: Spain, Ireland, Greece, Belgium, Luxemburg, Netherlands, France, Germany, Italy, and Finland.[2] The trade balance (tb_t) is the ratio of imports (M_t) to exports (X_t) of goods and services. The data for M_t and X_t are from the Eurostat database (chain linked volumes, index 2010 = 100). Since tb_t=M_t/X_t, a positive (negative) change in tb_t indicates a deterioration (improvement) of the trade balance.

[2] For Italy, the data available is for the period 1996:Q1-2019:Q4.

The real exchange rate (q_t) is the real effective exchange rate (REER), based on unit labor costs (ULC), with respect to the 37 main industrial countries. The real effective exchange rate for each country i is defined as:

$$q_{it} = \sum_j \omega_{ijt} e_{ijt} \frac{ULC_{it}}{ULC_{jt}} \tag{3}$$

where j denotes the trading partners, ω_{ij} are the bilateral trade weights in period t, e_{ijt} are the bilateral nominal exchange rates, and ULC_{it}/ULC_{jt} are the bilateral relative unit labor costs (or relative efficiency wages), defined as the ratio of average labor costs (nominal wage rate) to labor productivity:

$$ULC_t = \frac{w_t}{Y_t/E_t} \tag{4}$$

where w_t is the average nominal wage rate; Y_t is real gross domestic product at market prices (in millions, chain-linked volumes, base year 2010); and E_t indicates total employment (all industries, in number of persons). It includes both employees and the self-employed. Because of how q_{it} is constructed, a positive (negative) change in it denotes an appreciation (depreciation) of the real effective exchange rate of country i. Thus, a positive correlation between q and tb is expected. The data on the REER based on ULC is provided by Eurostat, and its unit is the Index 2010 = 100.

Figure 2 shows the trade balance and the real effective exchange rate of the ten countries under study. We can appreciate a progressive increase in the trade deficits of Greece and Italy since 1995. Spain started experiencing a progressive increase in its deficit after the euro was launched in 1999. This increasing deficit lasted until

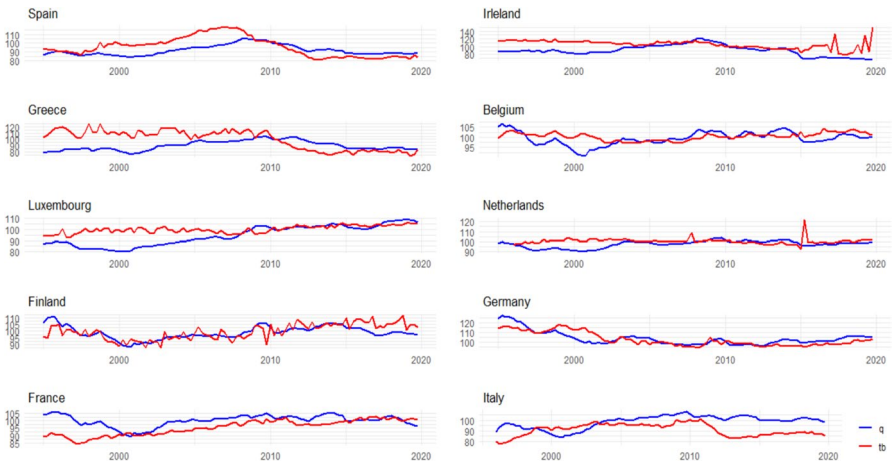

Fig. 2 Real effective exchange rate (q_t) and trade balance (tb_t). 2010 = 100. $tb_t M_t X_t tb_t M_t / X_t$ Source: Authors' elaboration based on Eurostat quarterly data. Notes: (i) Trade balance () is the ratio of imports () to exports () of goods and services (=). Exports and imports are measured in Chain linked volumes, index 2010 = 100 (seasonally and calendar adjusted data); (ii) Real effective exchange rate, Index 2010 = 100

Table 1 Descriptive statistics and unit root tests

Δtb_t							
Countries	Mean	Std.Dev	Skewness	Kurtosis	Jarque–Bera	ADF	PP
Spain	−0,054	2,85	0,41	2,00	6,68**	−2,80	−61,68***
Ireland	0,076	5,51	−0,05	9,78	201,16***	−5,33***	−162,89***
Greece	−0,20	12,94	0,42	1,66	10,08***	−5,36***	−60,30***
France	0,04	0,69	0,24	3,05	1,06	−4,25***	−131,11***
Italy	0,01	2,27	−0,08	1,89	4,81*	−4,14***	−64,81***
Belgium	0,01	0,62	−0,14	4,18	7,01**	−5,84***	−147,98***
Luxembourg	0,05	1,45	−0,28	4,54	12,40***	−9,09***	−129,41***
Netherlands	0,02	2,09	1,53	20,26	1328,84***	−7,14***	−111,53***
Germany	−0,03	1,31	−0,14	2,51	1,10	−4,97***	−102,22***
Finland	0,01	2,32	0,47	5,05	22,93***	−5,14***	−123,25***
Δq_t							
Countries	Mean	Std.Dev	Skewness	Kurtosis	Jarque–Bera	ADF	PP
Spain	0,01	0,44	−0,07	2,65	0,45	−3,76**	−57,17***
Ireland	−0,12	1,05	−1,03	6,38	68,91***	−4,09***	−43,96***
Greece	0,03	0,70	−0,11	3,16	0,44	−4,46***	−64,36***
France	−0,03	0,47	−0,07	2,59	0,59	−4,32***	−69,47***
Italy	0,07	0,71	0,28	6,62	59,54***	−5,13***	−100,36***
Belgium	−0,02	0,44	−0,06	2,99	0,08	−4,90***	−67,91***
Luxembourg	0,09	0,42	−0,02	3,50	1,35	−4,50***	−51,32***
Netherlands	0,00	0,39	−0,21	3,11	0,85	−4,58***	−71,77***
Germany	−0,07	0,56	−0,08	2,82	0,17	−4,75***	−77,09***
Finland	−0,04	0,61	−0,21	3,35	1,47	−4,37***	−63,87***

Source: Authors; ADF: Augmented Dickey-Fuller; PP: Phillips-Perron. The number of observations for each series is 99, and ***, **, and * refer to the rejection of the null hypothesis at the 1%, 5%, and 10% significance level, respectively

the Great Recession. From this moment onwards, these three countries reduced their trade deficits, and Spain and Italy attained a surplus. The situation of the core European countries is different. They experimented a progressive improvement in their trade balances since 1995, with a sole interruption in 2009.

For empirical purposes, we use the continuously compounded growth rates of q_t and tb_t, i.e., $\Delta q_t = \log(q_t/q_{t-1}) \times 100$ and $\Delta tb_t = \log(tb_t/tb_{t-1}) \times 100$. Table 1 shows the descriptive statistics (mean, maximum and minimum values, standard deviation, skewness, and kurtosis) of the series. It also shows the Jarque–Bera (J-B) normality test, and unit root tests of the variables in log-first differences, i.e., growth rates (denoted as Δ). The ADF and PP unit root tests conducted on q_t and tb_t reveal that both variables are non-stationary in levels.[3] However, the tests indicate that both variables in first differences, i.e., Δq_t and Δtb_t, are stationary.Since stationarity is a

[3] The test results are not presented here to save space; but they are available upon request.

necessary condition to test the null hypothesis of no Granger causality (see Hamilton 1994, Sect. 11.2), we apply the causality analysis to the first-differenced series.

On the other hand, the high J-B values presented in Table 1 reveal that Δtb_t of most counties is not normally distributed, and a few of the J-B values of Δq_t provide evidence of non-normality. The Δtb_t of France and Belgium, and the Δq_t of Greece, Luxembourg, Netherlands, and Finland exhibit high kurtosis, which indicates that these variables exhibit frequent extreme events. Our methods deal with nonlinearity and incorporate the role of asymmetry and other sources of nonlinearity, such as regime changes, time varying effects, and changing interactions across time horizons.

3 Econometric Methodology

The first step is to test whether the relationship between Δtb_t and Δq_t is linear against the alternative of nonlinear. We use the BDS test of Brock et al. (1996). The results of the test (Table 2) reject the null hypothesis and indicate that the relationship between the variables is nonlinear. This results is in line with the findings of Nogueira and León-Ledesma (2011), who suggest that exchange rates pass-through into consumer prices are nonlinear. This result implies that the relationship between the exchange rate and the trade balance must be analyzed by means of nonlinear econometrics.

3.1 Time-domain causality tests

Standard Granger-causality tests (Granger 1969) assume that the parameters of the vector autoregressive (VAR) model are constant over time. However, time series data usually exhibit structural changes that the standard Granger-causality tests do not capture. Researches can identify and incorporate structural changes by splitting the sample and by adding dummy variables, but these procedures introduce pretest bias. In order to overcome the possible parameter non-constancy and avoid pretest bias, we adopt both quantile Granger-causality and rolling-window Granger-causality approaches. The Appendix provides some details of the tests. In what follows, we outline the time series techniques that we use to study the nexus between Δtb_t and Δq_t within the time-domain approach.

Since Granger-causality tests in mean overlook the possible relationships in the conditional tails of the distribution, we first test for Granger causality across different quantiles of the conditional distribution. Quantile Granger causality tests examine if the causal relationship between Δq_t and Δtb_t is asymmetric across the distribution. In order to consider the role of regimes in the dependent variable, we first use the parametric approach of Troster (2018) to test for Granger-noncausality in conditional quantiles. It allows to identify the pattern of causality and provides a sufficient

Table 2 BDS test results

	BDS test for Δq_t(p-value)									
Dimension	Belgium	Netherlands	Finland	Luxemburg	Ireland	Spain	Greece	France	Germany	Italy
2	0,00	0,00	0,00	0,00	0,00	0,00	0,00	0,00	0,00	0,00
3	0,00	0,00	0,00	0,00	0,00	0,00	0,00	0,00	0,00	0,00
4	0,00	0,00	0,00	0,00	0,00	0,00	0,00	0,00	0,00	0,00
5	0,00	0,00	0,00	0,00	0,00	0,00	0,00	0,00	0,00	0,00
6	0,00	0,00	0,00	0,00	0,00	0,00	0,00	0,00	0,00	0,00
	BDS test for Δtb_t(p-value)									
Dimension	Belgium	Netherlands	Finland	Luxemburg	Ireland	Spain	Greece	France	Germany	Italy
2	0,00	0,03	0,00	0,00	0,00	0,00	0,00	0,00	0,89	0,13
3	0,00	0,00	0,00	0,00	0,00	0,00	0,45	0,00	0,94	0,00
4	0,00	0,00	0,00	0,00	0,00	0,00	0,54	0,00	0,35	0,00
5	0,00	0,00	0,00	0,00	0,00	0,00	0,00	0,00	0,01	0,00
6	0,00	0,00	0,00	0,00	0,00	0,00	0,00	0,01	0,00	0,00

This table presents the results of the BDS test on Δtb_t and Δq_t.

condition for Granger causality. Let assume that $Q_{\tau}^{\Delta tb,\Delta q}\left(\cdot|I_t^{\Delta tb}, I_t^{\Delta q}\right)$ denotes the τ -quantile of $F_{\Delta tb}\left(\cdot|I_t^{\Delta tb}, I_t^{\Delta q}\right)$. Then, the null hypothesis of no Granger causality is:

$$H_0^{QC:\Delta q \nrightarrow \Delta tb} : Q_{\tau}^{\Delta tb,\Delta q}\left(\Delta tb_t|I_t^{\Delta tb}, I_t^{\Delta q}\right) = Q_{\tau}^{\Delta tb}\left(\Delta tb_t|I_t^{\Delta tb}\right), \text{for all } \tau \in \mathcal{T}. \quad (5)$$

Following Ahmed et al. (2020), we use the nonlinear conditional autoregressive value-at-risk (CAViaR) models of Engle & Manganelli (2012) under the null. The CAViaR models specify an autoregressive process of the quantiles and obtain reliable more reliable results than alternative methods (see Troster et al. 2018).

Second, we apply the nonparametric causality-in-quantile test of Balcilar et al. (2017). To the best of our knowledge, this is the first article in the exchange rate-trade balance nexus literature that uses a nonparametric Granger causality method. The nonparametric test of Balcilar et al. (2017) is a model-free method, robust to the misspecification of the quantile regression. The method also accounts for the existence of possible outliers and structural breaks. Based on Jeong et al. (2012), Balcilar et al. (2017) overcome the problem of the difference between causality in mean and causality in variance. The hypothesis of quantile Granger-causality from Δq_t to Δtb_t in higher-order moments is specified as:

$$H_0 = P\left\{F_{\Delta tb_t^K|W_{t-1}}\left\{Q_{\tau}(TB_{t-1})|W_{t-1}\right\} = \tau\right\} = 1 \; for \; k = 1, 2, \ldots, K \quad (6)$$

and the alternative as:

$$H_1 = P\left\{F_{\Delta tb_t^K|W_{t-1}}\left\{Q_{\tau}(TB_{t-1})|W_{t-1}\right\} = \tau\right\} < 1 \; for \; k = 1, 2, \ldots, K, \quad (7)$$

where $\mathrm{TB}_{t-1} \equiv (\Delta \mathrm{tb}_{t-1}, \ldots, \Delta \mathrm{tb}_{t-p})$, and $\mathrm{W}_{t-1} \equiv \left(\Delta \mathrm{tb}_{t-1}, \ldots, \Delta \mathrm{tb}_{t-p}, \Delta \mathrm{q}_{t-1}, \ldots, \Delta \mathrm{q}_{t-p}\right)$.

Finally, we also use a rolling-window Granger-causality test, specifically the Hacker and Hatemi-J (2012) time-varying approach. This test relies on fixed-size subsamples rolling sequentially from the beginning to the end of the sample by adding one observation from ahead and dropping one from behind. The test is applied to each subsample, instead of estimating a single causality test for the entire sample. Possible changes in the causal linkages between the variables can be intuitively identified by calculating the bootstrap p-values of observed LR statistics rolling through the subsamples. The test is based on the lag-augmented VAR (LA-VAR) model specification of Kurozumi and Yamamoto (2000):

$$Y = DZ + \delta \quad (8)$$

In Eq. (8), $Y := (y_1, y_2, ..., y_T)$ refers to an $(n \times T)$ matrix in which n is the number of variables and T is the sample size. In this framework, $D := (\alpha, A_1, A_2, ..., A_k)$ is an $(n \times (1 + (k + d_{\max}))$ matrix and $Z := (Z_0, Z_1, ..., Z_{T-1})$ denotes a $\left(\left(1 + n\left(k + d_{\max}\right)\right) \times T\right)$ matrix. Thus, a matrix can be written as:

$$Z_t := \begin{bmatrix} 1 \\ y_t \\ y_{t-1} \\ \cdot \\ \cdot \\ y_{t-k+1} \end{bmatrix},$$

and $\delta := \left(u_1, u_2, ..., u_T\right)$ represents a $(n \times T)$ matrix. Equation (A16) constitutes a framework test for the null of no causality. The null hypothesis of Granger-noncausality is:

$$H_0 : C\beta = 0 \tag{9}$$

and can be tested through the following Wald statistic:

$$Wald = (C\beta)' \left[C\left(\left(Z'Z \right)^{-1} \otimes S_u \right) C' \right]^{-1} (C\beta) \sim X_p^2 \tag{10}$$

where $\beta = vec(D)$, *vec* is the column-stacking operator, $\otimes$ is the Kronecker product, C is a $(\mathrm{p} \times \mathrm{n})(1 + \mathrm{p} \times \mathrm{n})$ indicator matrix with ones and zeros, and S_u is the variance–covariance matrix of the unrestricted VAR model. Additionally, we incorporate the role of asymmetry in the rolling-window Granger causality framework. This is important because it allows us to separately study if depreciations (appreciations) Granger-cause improvements (deteriorations) in the trade balance.

3.2 Combined Time- and frequency-domain tests

We also investigate how Δq_t and Δtb_t are related at different frequencies and how this relationship changes over time. We conducted two tests. The Appendix provides details of the tests. We start the time- and frequency-domain analyses by applying the partial wavelet coherence (PWC) approach to capture the co-movement of Δq_t and Δtb_t. This is a non-parametric method that allows the decomposition of a time series into the bi-dimensional time–frequency sphere. As suggested by Granger (1969), the strength and direction of causal relationships among variables may vary over different frequencies. Fourier transformations (FT) can be used to focus on the frequency domain of the variables. However, FT do not provide information on how the frequency components of the time series change over time. Therefore, time information is lost. This means that Fourier analysis is not appropriate to analyze time-varying relationships between economic variables. Wavelet analysis overcomes this problem by incorporating both the frequency and the time-varying features of a series. The advantage of wavelet analysis over FT is that it considers time domain as well as frequency domain. For these reasons, we use wavelet analysis. This permits

the analysis of the long- and the short-run causal linkages between Δq_t and Δtb_t across different time scales.

The Wavelet Coherence (WC) of two series $\Delta q = \{\Delta q_n\}$ and $\Delta tb = \{\Delta tb_n\}$ is the localized correlation coefficient among these variables in the time–frequency domain. We calculate the WC as the squared absolute value of the smoothed cross wavelet spectrum normalized by the product of the smoothed individual wavelet partial spectrum of each variable:

$$R^2(u,s) = \frac{\left|S\left(s^{-1}W_{\Delta q \Delta tb}(u,s)\right)\right|^2}{S\left(s^{-1}\left|W_{\Delta q}(u,s)\right|^2\right)S\left(s^{-1}\left|W_{\Delta tb}(u,s)\right|^2\right)} \tag{11}$$

where for each signal Δq and Δtb, the individual wavelet spectra is $W_n^{\Delta q}(s)$ and $W_n^{\Delta tb}(s)$. The Cross-Wavelet between two signals is expressed as $CWS_n^{\Delta q \Delta tb}(s) = W_n^{\Delta q}(s)W_n^{\Delta tb^*}(s)$, where $W_n^{\Delta tb^*}$ is the complex conjugate of $W_n^{\Delta tb}(s)$. The CWP is thus defined as $\left|W_n^{\Delta q \Delta tb}\right|$. The Wavelet Coherence (WC) of two series $\Delta q = \{\Delta q_n\}$ and $\Delta tb = \{\Delta tb_n\}$ is the localized correlation coefficient among these variables in the time–frequency domain. We calculate WC as the squared absolute value of the smoothed CWS normalized by the product of the smoothed individual WPS of each variable.

Finally, we use the newly proposed Wavelet Quantile Correlation (WQC) technique to identify the degree and sign of correlation between the variables considering the role of regimes and the frequency domain. The WQC procedure is a notable extension of the quantile correlation estimator inspired by Percival and Walden (2000) and Li et al. (2015). The WQC estimator allows information identification over different quantiles and time horizons. The model also considers tail and structure dependence across differing time dimensions. Likewise, the WQC procedure allows the study of the dynamic dependence structure over varying time scales. Additionally, the procedure adequately captures the potentiality of asymmetric association among the series and over their distributions. The quantile correlation method is implemented by Kumar and Padakandla (2022) by means of a maximal overlapping discrete wavelet transform to decompose Δq_t and Δtb_t. Pairs of Δq_t and Δtb_t are decomposed at the j_{th} level, and quantile correlation techniques are applied to get the wavelet quantile correlation for each level j. The wavelet quantile correlation is:

$$WQC_t(\Delta tb, \Delta q) = \frac{QC_t(d_j[\Delta tb], d_j[\Delta q])}{\sqrt{var(\theta_\tau(d_j[\Delta tb] - Q_{\tau,d_j[\Delta tb]}))var(d_j[\Delta q])}} \tag{12}$$

where $Q_{\tau,\Delta q}$ is the τ-th quantile of Δq, and $Q_{\tau,\Delta tb}(\Delta q)$ the τ-th quantile of Δtb conditioning on Δq.

4 Empirical Results

This section summarizes our results. For reasons of space, we only present the results of the causality tests running from Δq to Δtb since the purpose of the paper is to identify the causal effects of depreciations and appreciations on the trade balance:

(i) As stated above, to implement the Granger causality test in quantiles of Troster (2018), we specify nonlinear CAViaR models under the null of no Granger-causality (see Ahmed et al. 2022).[4] We compare the root mean squared error (RMSE) of 120 recursive out-of-sample forecasts of the quantiles $\tau = \{0.05–0.95\}$ of the distribution of Δtb_t. We find that the nonlinear CAViaR models overall outperform linear quantile models. This justifies using these specifications to test for Granger causality in quantiles between Δq_t and Δtb_t. Nevertheless, results do not qualitatively change if we use the linear quantile autoregressive (QAR) models instead of the nonlinear specifications. Table 3 shows the results, which indicate no evidence of causality from Δq_t to Δtb_t at any quantile of the conditional distribution of Δtb_t.

(ii) Given the lag-dependence of the Granger causality found through the Troster (2018) test, we also applied the model-free Granger-causality in quantiles test of Balcilar et al. (2017).[5] Figure 3 shows the results of the Balcilar et al. (2017) non-parametric Granger-causality in quantiles test in mean between Δq_t and Δtb_t. The vertical axis shows the test statistic for each quantile (shown in the horizontal axis). The 5% critical value is 1.96 and the 10% critical value is 1.64. Lower, middle and higher quantiles (in the horizontal axis), relate to stuck, normal and booming periods/conditions of the trade balance. Figure 3 indicates that, except for Spain, all test statistics are below the critical value of 10% across all quantiles of the conditional distribution of Δtb_t. Thus, for Spain, Δq_t Granger-causes Δtb_t over the quantile range of 0.30–0.40. This suggests that changes in q_t cause changes in tb_t in the middle-lower tails of the conditional distribution of Δtb_t, but not in the extreme tails. In other words: Δq_t helps predict Δtb_t in *normal* times, but not in booms of the trade balance such as the one experienced by Spain after the Great Recession. Overall, these results are in line with those of the parametric Granger causality in quantiles test of Troster (2018), suggesting sparse evidence of causality from Δq_t to Δtb_t.

(iii) Since we have found evidence of Granger causality from Δq_t to Δtb_t at some quantiles of the conditional distribution of Δtb_t for Spain, we apply the rolling-window Granger-causality test of Hacker and Hatemi-J (2012) to this country.[6] Since the rolling-window Granger causality framework allows for time-varying effects, we can identify the periods in which depreciations (appreciations) have Granger-caused improvements (deteriorations) in the trade balance in Spain.[7]

[4] We used the Matlab code provided by Ahmed et al. (2022).

[5] Professor Balcilar kindly provided us with the R code to implement this test.

[6] We used the Gauss code provided by Yilanci and Kilci (2021).

[7] We also applied the test to the other countries and did not find any evidence of causality. Results are not presented to save space, but they are available upon request.

Table 3 Nonlinear quantile-causality from Δq_t to Δtb_t (CAViaR models)

τ	Spain		Ireland		Greece		France		Italy		Netherlands		Belgium		Finland		Luxemburg		Germany	
	SAV	AS	SAV	AS	SAV	AS	SAV	AS	SAV	AS	SAV	AS	SAV	AS	SAV	AS	SAV	AS	SAV	AS
0,05	0,06	0,03	1,00	1,00	0,30	0,12	0,06	1,00	0,21	0,12	0,06	1,00	1,00	1,00	0,15	1,00	1,00	**0,03***	1,00	1,00
0,10	0,18	0,91	0,36	0,49	0,91	0,64	0,55	0,39	1,00	0,48	0,48	0,39	0,36	0,39	0,27	0,61	0,42	0,52	0,58	0,39
0,15	0,15	0,09	0,58	1,00	1,00	0,76	0,55	1,00	1,00	1,00	1,00	0,58	1,00	0,58	1,00	0,61	0,58	0,24	1,00	1,00
0,20	**0,03***	**0,03***	0,15	0,42	0,03*	0,67	0,36	0,55	0,45	0,36	0,21	0,15	0,45	0,15	0,52	0,48	0,52	0,58	0,55	0,42
0,25	**0,03***	0,09	0,49	0,21	0,27	0,09	0,42	0,36	0,21	0,21	0,58	0,55	0,48	0,55	0,39	0,39	0,52	0,21	0,48	0,48
0,30	0,12	0,12	0,46	0,36	0,09	0,21	1,00	1,00	0,12	0,06	0,55	1,00	0,39	1,00	0,58	1,00	1,00	1,00	1,00	0,55
0,35	0,48	0,36	0,52	0,33	0,18	0,97	0,52	0,49	0,33	0,06	0,45	0,55	0,39	0,55	0,52	0,52	0,48	0,15	0,39	0,64
0,40	0,45	0,52	0,18	0,82	0,73	0,24	0,42	0,46	0,06	0,03	0,12	0,64	1,00	0,64	1,00	0,67	1,00	1,00	1,00	0,36
0,45	0,24	0,48	0,67	0,58	0,70	0,21	0,58	0,55	**0,03***	0,09	0,39	0,48	0,48	0,48	0,70	0,55	0,61	0,48	0,61	0,55
0,50	0,12	0,12	0,30	0,12	0,33	0,21	0,09	1,00	0,42	0,09	1,00	0,21	0,15	0,21	1,00	0,09	1,00	0,21	0,15	1,00
0,55	0,27	0,06	0,46	0,70	0,18	0,27	0,52	0,58	0,33	0,24	0,85	0,76	0,36	0,76	0,79	0,45	0,55	0,67	0,36	0,45
0,60	0,06	0,12	0,42	0,39	0,79	0,64	0,58	1,00	0,06	0,12	0,52	0,36	1,00	0,36	1,00	1,00	0,61	1,00	0,52	1,00
0,65	0,39	**0,03***	0,61	0,61	0,82	0,24	0,39	0,49	0,09	0,12	0,42	0,48	0,73	0,48	0,52	0,55	0,39	0,61	0,42	0,64
0,70	0,09	0,12	0,21	0,58	0,70	0,58	1,00	1,00	0,88	0,24	0,61	1,00	1,00	1,00	0,39	0,12	0,03*	1,00	1,00	0,52
0,75	0,06	0,09	0,55	0,67	0,33	0,15	0,49	0,55	0,30	0,52	0,45	0,64	0,55	0,64	0,58	0,42	0,61	0,48	0,39	0,18
0,80	0,06	0,24	0,42	0,64	0,06	**0,03***	0,46	0,55	0,45	0,27	0,48	0,45	0,42	0,45	0,70	0,67	0,42	0,18	0,45	0,45
0,85	**0,03***	0,06	1,00	0,70	0,39	**0,03***	0,39	1,00	0,30	0,88	0,64	1,00	0,21	1,00	1,00	0,48	1,00	0,24	1,00	1,00
0,90	0,58	0,27	0,46	0,46	0,21	**0,03***	0,52	0,49	0,21	0,48	0,39	0,27	0,48	0,27	0,45	0,55	0,33	0,52	0,42	0,42
1	0,18	0,67	1,00	0,24	0,79	0,15	0,09	1,00	0,73	0,09	**0,03***	0,15	1,00	0,15	1,00	0,12	0,21	0,18	1,00	1,00

Source: Authors

This table shows the subsampling *p*-values of the CAViaR tests. The asterisk * indicates rejection of the null hypothesis of no Granger causality at the 5% significance level. SAV is the symmetric absolute value model, while AS is the asymmetric slope model

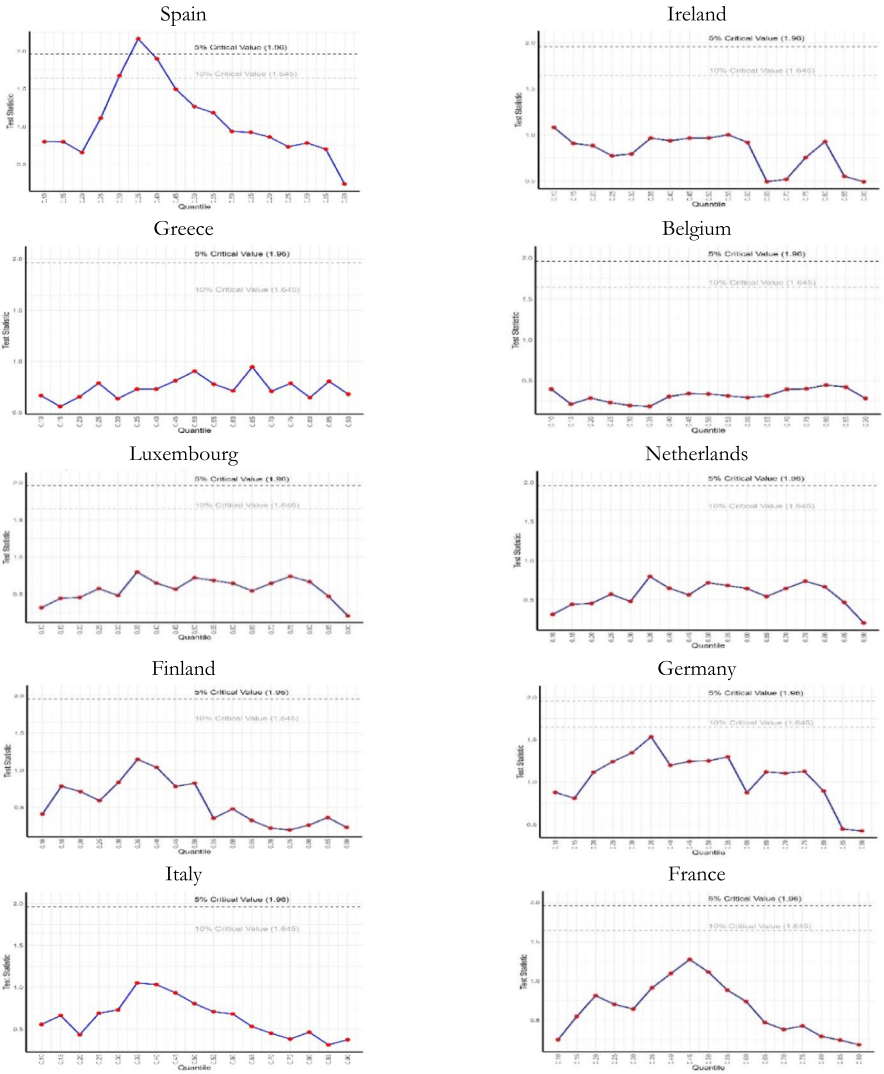

Fig. 3 Balcilar (2017) non-parametric quantile Granger causality from Δq_t to Δtb_t. Source: Authors

Figure 4 shows the results of the time-varying bootstrap causality test. The horizontal axis depicts the time-period, while the *p*-values obtained by the test are measured along the vertical axis. The graph at the top of the figure shows the results of the Granger causality test from appreciations (Δq_t^+) to deteriorations in the trade balance (Δtb_t^+); while the graph at the bottom shows the results of the Granger causality test running from depreciations (Δq_t^-) to improvements in the trade balance (Δtb_t^-). We observe that the p-value is below 5% only in very few moments of the time-span under study. Thus, we find sparse empirical support for the argument that changes in the real exchange rates predict changes in the

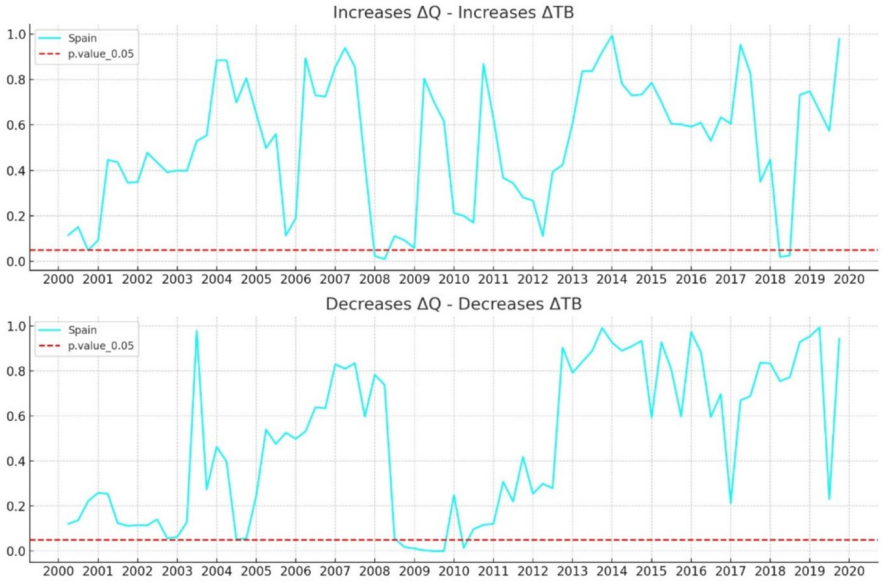

Fig. 4 Hacker and Hatemi-J (2012) rolling-window Granger causality for Spain. Source: Authors

trade balances. Figure 4 indicates that depreciations contributed to the improvement of the trade balance in Spain only at the beginning of the Great Recession. Overall, the results of the time-varying bootstrap Granger causality are in line with the Granger causality in quantiles tests, indicating sparse evidence of causality from exchange rate changes to trade balance changes.

(iv) We next test the causal relationship between Δq_t and Δtb_t in the time–frequency domain by means of the partial wavelet coherency (PWC) framework.[8] Compared to the time-domain approach, this method provides a better understanding of the nature of the lead-lag relationship between Δq_t and Δtb_t insofar as it allows to study the frequency components of the time series without losing the time information.

Figure 5 shows the wavelet coherence plots, which provide information about the magnitude of the effect that a shock in one variable has on the other one. We display the mean values for the phase-differences and partial gains corresponding to the two frequency bands considered, namely for cycles of $9 \sim 16$ and $22 \sim 28$ quarters. We measure the phase-differences on a circular scale and compute their mean as a circular one. Each wavelet measure is a function of t (time) and s (scale or frequency). The wavelet power and the wavelet coherencies are plotted as 2-dimensional heat-maps, with colors ranging from blue (low power/small coherency) to yellow (high power/high coherency). The black contours show the

[8] To construct the wavelet coherence plots, we used the Matlab code from https://grinsted.github.io/wavelet-coherence/.

Fig. 5 Wavelet coherence plots. $\Delta tb_t \Delta q_t$ Source: Authors. Note: Phase arrows indicate the direction of co-movement between and. The thick black contour lines indicate the 5% significance intervals estimated from Monte Carlo simulations with phase randomized surrogate series. The cone of influence, which marks the region affected by edge effects, is shown with a lighter shade black line. The color legend for spectrum power ranges from Blue (low power) to yellow (medium power) and red (high power). Y-axis measures frequency (scale) and X-axis represents the time period ▶

5% significance level of co-movements between Δtb_t and Δq_t, derived from an ARMA (1, 1) model. We measure the time-period along the x-axis and the frequency (scale) along the y-axis. Thus, the plot clearly identifies both frequency bands and time intervals where the series move together.

Figure 5 also shows the relative phasing of the variables by means of phase arrows, which indicate the direction of interdependence and cause–effect relationships. Arrows pointing to the left indicate that the variables are in phase (positive correlation), while arrows pointing to the right indicate that the variables are in antiphase (negative correlation). If the arrows point to the right and up, then the phase-difference lies between 0 and $\pi/2$, and both series move in the phase but the former variable (Δtb_t) leads the latter (Δq_t). If the arrows point to the right and down, the phase-difference lies between $-\pi/2$ and 0, and then Δq_t leads Δtb_t. If the arrows point to the left and up, the partial phase-difference lies within the range $(\pi/2; \pi)$, which means that Δq_t leads Δtb_t. Finally, if the arrows point to the left and down, the phase-difference lies within $(-\pi; -\pi/2)$ and Δtb_t leads Δq_t. Therefore, the condition for same-sign causality from Δq_t to Δtb_t is that the phase-difference between Δtb_t and Δq_t in the regions of high partial coherence lie between $\pi/2$ and π, i.e., arrows point to the left and up.

First, the multiple directions of the arrows indicate that the interdependence between Δq_t and Δtb_t is not homogeneous across different times and scales. Second, we see that for Spain, Δq_t positively leads Δtb_t for the time scale of 3–5-quarter frequency band for 2016–2019; and for Greece, Δq_t positively leads Δtb_t for the time scale of 10–14-quarter frequency band for 2002–2007. For the rest of the countries, however, there is no evidence of a same-sign causal relationship between changes in exchange rate and trade balance. This result is in line with the results of the time-domain analysis and conflicts with the hypothesis of an overall significant exchange rate-trade balance causal nexus in European countries.

(v) Finally, we applied the newly proposed WQC technique of Li et al. (2015).[9] The WQC procedure is a notable extension of the quantile correlation estimator inspired by Percival and Walden (2000). Figure 6 shows the results. We extract information at the scales of 2–4 quarters, 4–8 quarters (short run), 8–16 quarters (medium run), and 16–32 quarters (long run). The deep black color boxes denote a negative quantile correlation between the variables. Conversely, the highly yellow color boxes represent a positive association, denoting the exchange rate's same-sign effects on the trade balance.

[9] We used the R code provided by Kumar and Padakandla (2022).

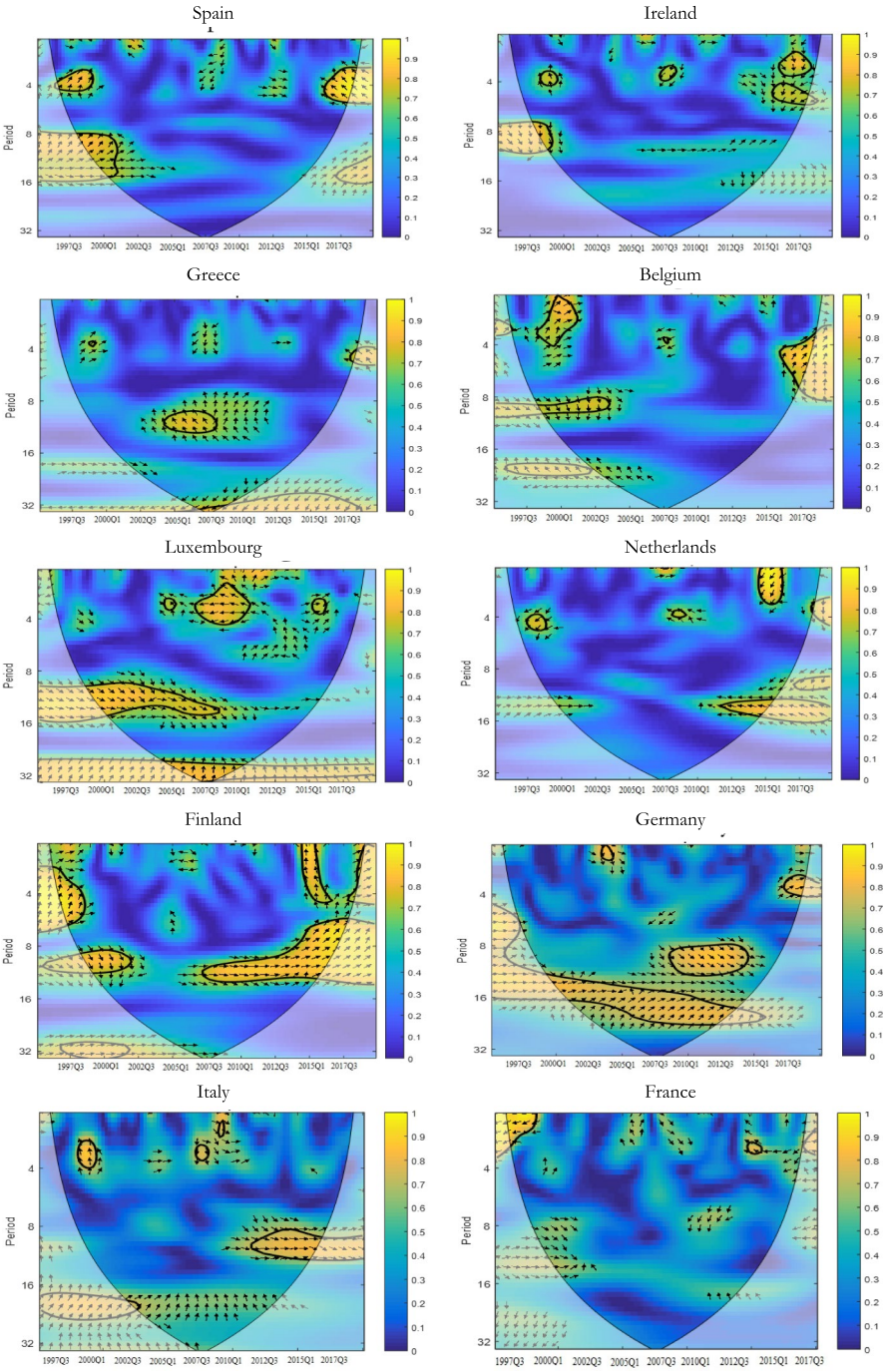
Spain
Ireland
Greece
Belgium
Luxembourg
Netherlands
Finland
Germany
Italy
France
Period
4
8
16
32
1997Q3
2000Q1
2002Q3
2005Q1
2007Q3
2010Q1
2012Q3
2015Q1
2017Q3
0
0.1
0.2
0.3
0.4
0.5
0.6
0.7
0.8
0.9
1

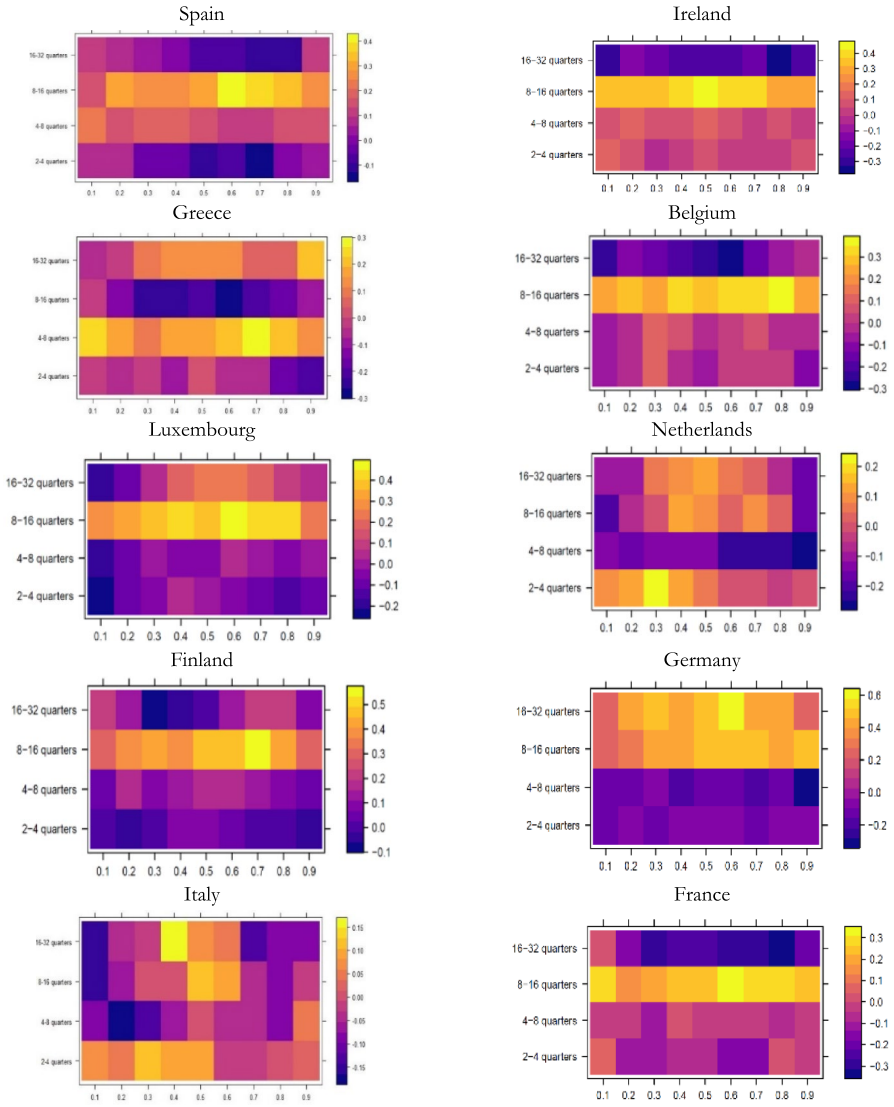

Fig. 6 Wavelet Quantile Correlation (WQC). Source: Authors

In Fig. 6 we can see that the quantile correlation between Δq_t and Δtb_t reveals varying correlation across the quantile distributions of Δtb. Above all, we observe positive correlation coefficients in all countries, but they are not sufficiently high to conclude that the variables are dynamically connected. The exception is Germany, which presents a relevant positive association between Δq_t and Δtb_t at medium quantiles in the long run. For this country, we observe a sort of J-curve relationship (Magee 1973) between Δq_t and Δtb_t, since the

variables are negatively (positively) correlated in the short run (long run). On the other hand, at some quantile and time frequencies, we observe that the variables are negatively correlated (despite the coefficient of correlation not being so significant) in the long run for Spain, Ireland, Belgium, Luxemburg, Finland and France. This result might partly align with the theoretical and empirical literature indicating contractionary effects of currency devaluation (Krugman and Taylor 1978; Fukui et al. 2023).

5 Conclusions

This paper has used time and frequency-domain tests to analyze if depreciations (appreciations) of the real effective exchange rate based on unit labor costs caused improvements (deteriorations) in the trade balance in Spain, Ireland, Italy, Greece, Belgium, Luxemburg, Netherlands, Germany, France, and Finland, during 1995–2019.

The time-domain tests used in this paper have several advantages: (i) they are robust to parameter instability/structural breaks; (ii) they consider nonlinear effects and discriminate between negative and positive shocks; and (iii) they allow eliminating the variations related to the seasonal pattern present in macroeconomic series. Within the time-domain approach, we have found no evidence of a clear pattern of causality from depreciations (appreciations) to improvements (deteriorations) in the trade balance. We have also tested the relationship between the exchange rate and the trade balance using a frequency-domain approach. This allows for non-linearities and causality cycles, i.e., causality at high, intermediate, or low frequencies, thereby differentiating between causality in the short, medium, and long run.

The tests we have implemented are more powerful than conventional causality tests. Yet, we have not identified causality running from changes in the exchange rate to changes in the trade balance in the European countries under study. Our results indicate that trade imbalances among Euro countries have not been corrected as a result of changes of the exchange rate. In line with Bajo-Rubio et al. (2016), Xifré (2017), and Bilbao-Ubillos and Fernández-Sainz (2019, 2022), our results suggest that, overall, the trade balances of the Euro Zone economies do not depend much on prices and costs. This means that other factors, such as the increasing participation of countries in global value chains, market accessibility, market size, Ricardian technological advantage, and the institutional and political framework, are possibly more determinant. These will be the subject of future research.

Overall, our results also stress the importance of working within a nonlinear approach to study the relationship between the exchange rate and the trade balance (as shown by the BDS test). Since the literature has widely recognized that macroeconomic variables and processes have nonlinear structures, the information obtained from linear models might not be enough to reliably forecast. Shin et al. (2014) warn that the assumption of linear adjustments may be too restrictive in many economically interesting situations, especially when transaction costs are important and

where policy interventions are observed in-sample. In our case, the adjustment process has proven to be nonlinear for some countries.

This study has several limitations that should be acknowledged to inform future research directions. Expanding the sample to encompass both Eurozone and non-Eurozone economies would offer a more comprehensive perspective on the role of exchange rates in trade balance adjustment mechanisms. Furthermore, various macroeconomic factors such as domestic and international economic conditions, global commodity price shocks, trade policy measures, and supply chain disruptions, may have influenced trade balance dynamics but were not explicitly accounted for in this analysis.

Future methodological refinements could enhance the robustness of our findings. Markov-switching models or nonlinear autoregressive distributed lag (ARDL) models may facilitate the identification of critical exchange rate thresholds at which trade balance adjustments become significant. Additionally, distinguishing between final and intermediate goods would improve the granularity of exchange rate effects on trade balances, particularly in light of the increasing prominence of global production networks. Finally, this study does not explicitly incorporate policy-driven factors, thereby limiting its direct policy implications. Future research should examine trade balance dynamics within the broader context of financial market fluctuations, capital flows, and the interplay between exchange rates and trade balances in environments characterized by geopolitical risks and policy uncertainty. Furthermore, sectoral-level analyses could provide valuable insights into whether specific industries exhibit heterogeneous sensitivities to exchange rate movements.

Appendix: Causality Tests Implemented

A series x_t is said to Granger-cause another variable y_t if past values of $\mathrm{x_t}$ help forecast future values of y_t beyond the information provided by past values of y_t. We test the null hypothesis of Granger-noncausality from Δq_t to Δtb_t as:

$$H_0^{\Delta q \nrightarrow \Delta tb} : F_{\Delta tb}\left(\Delta tb | I_t^{\Delta tb}, I_t^{\Delta q}\right) = F_{\Delta tb}\left(\Delta tb | I_t^{\Delta tb}\right)\varepsilon, for\ all\ \Delta tb \in \mathbb{R}, \varepsilon \quad \text{(A1)}$$

where $I_t \equiv (I_t^{\Delta tb}, I_t^{\Delta q})' \in \mathbb{R}^d$, where $\mathrm{I_t^{\Delta tb}}$ and $\mathrm{I_t^{\Delta q}}$ denote the past information sets of $\mathrm{\Delta tb_t}$ and $\mathrm{\Delta q_t}$, and $\mathrm{F_{\Delta tb}\left(\cdot | I_t^{\Delta tb}, I_t^{\Delta q}\right)}$ is the conditional distribution function of $\mathrm{\Delta tb_t}$ given $(\mathrm{I_t^{\Delta tb}}, \mathrm{I_t^{\Delta q}})$.

Time Domain Tests

Troster (2018)

Once we build the null of (5), we then use three quantile auto-regressive (QAR) models m(·), for all $\tau \in \mathcal{T} \subset [0,1]$:

$$QAR(1) : m^1\left(I_t^{\Delta tb}, \theta(\tau)\right) = \mu_1(\tau) + \mu_2(\tau)\Delta tb_{t-1} + \sigma_t\Phi_u^{-1}(\tau) \tag{A2}$$

$$QAR(2) : m^2\left(I_t^{\Delta tb}, \theta(\tau)\right) = \mu_1(\tau) + \mu_2(\tau)\Delta tb_{t-1} + \mu_3(\tau)\Delta tb_{t-2} + \sigma_t\Phi_u^{-1}(\tau) \tag{A3}$$

$$QAR(3) : m^3\left(I_t^{\Delta tb}, \theta(\tau)\right) = \mu_1(\tau) + \mu_2(\tau)\Delta tb_{t-1} + \mu_3(\tau)\Delta tb_{t-2} + \mu_4(\tau)\Delta tb_{t-3} + \sigma_t\Phi_u^{-1}(\tau), \tag{A4}$$

where the parameters $\theta(\tau) = (\mu_1(\tau), \mu_2(\tau), \mu_3(\tau), \mu_4(\tau), \sigma_t)\prime$ are estimated with maximum likelihood in an equally-spaced grid of quantiles. $\Phi_u^{-1}(\cdot)$ is the inverse of a standard normal distribution function, while the estimation of the quantile autoregressive models in Eq. (8) indicates the sign of the causal relationship among the variables.

Balcilar et al. (2017)

According to Jeong et al. (2012), the variable Δq_t does not Granger-cause the variable Δtb_t in the τ-th quantile if:

$$Q_\tau\left\{\Delta tb_t \middle| \Delta tb_{t-1}, \ldots, \Delta tb_{t-p}; \Delta q_{t-1}, \ldots, \Delta q_{t-p}\right\} = Q_\tau\left\{\Delta tb_t \middle| \Delta tb_{t-1}, \ldots \Delta tb_{t-p}\right\}, \tag{A5}$$

while Δq_t Granger-causes Δtb_t in the τ-th quantile if:

$$Q_\tau\left\{\Delta tb_t \middle| \Delta tb_{t-1}, \ldots, \Delta tb_{t-p}; \Delta q_{t-1}, \ldots, \Delta q_{t-p}\right\} \neq Q_\tau\left\{\Delta tb_t \middle| \Delta tb_{t-1}, \ldots \Delta tb_{t-p}\right\}, \tag{A6}$$

where $Q_\tau\{\Delta tb_t|\bullet\}$ is the τ-th quantile of Δtb_t. If $TB_{t-1} \equiv (\Delta tb_{t-1}, \ldots, \Delta tb_{t-p})$, $W_{t-1} \equiv (\Delta tb_{t-1}, \ldots, \Delta tb_{t-p}, \Delta q_{t-1}, \ldots, \Delta q_{t-p})$, and $V_t = (TB_t, W_t)$, then $F_{\Delta tb_t|W_{t-1}}(\Delta tb_t, W_{t-1})$ and $F_{\Delta tb_t|TB_{t-1}}(\Delta tb_t, TB_{t-1})$ are the conditional distribution functions of Δtb_t given TB_{t-1} and W_{t-1}, respectively. Jeong et al. (2012) assume that $F_{\Delta tb_t|W_{t-1}}(\Delta tb_t, W_{t-1})$ is absolutely continuous in Δtb_t for almost all V_{t-1}. If we denote $Q_\tau(W_{t-1}) \equiv Q_\tau(\Delta tb_t|W_{t-1})$ and $Q_\tau(TB_{t-1}) \equiv Q_\tau(\Delta tb_t|TB_{t-1})$, then the null hypothesis of no Granger causality from Δq_t to Δtb_t in the τ-th quantile is:

$$H_0 = P\left\{F_{\Delta tb_t|W_{t-1}}\left\{Q_\tau(TB_{t-1})\middle|W_{t-1}\right\} = \tau\right\} = 1, \tag{A7}$$

while the hypothesis that Δq_t Granger-causes Δtb_t in the τ-th quantile is:

$$H_1 = P\left\{F_{\Delta tb_t|W_{t-1}}\left\{Q_\tau(TB_{t-1})\middle|W_{t-1}\right\} = \tau\right\} < 1. \tag{A8}$$

Jeong et al. (2012) use the distance measure $J = \left\{\varepsilon_t E\left(\varepsilon_t|W_{t-1}\right)f_W(W_{t-1})\right\}$, where ε_t and $f_W(W_{t-1})$ are the regression error term and the marginal density function of W_{t-1},

respectively. Since ε_t is true only if $E\left[1\left\{\Delta tb_t \le Q_\tau(TB_{t-1})\middle|W_{t-1}\right\}\right] = 0$, Jeong et al. (2012) specify the distance function as:

$$J = E\left[\left\{F_{\Delta tb_t|W_{t-1}}\left\{Q_\tau(TB_{t-1})\middle|W_{t-1}\right\} - \tau\right\}^2 f_W(W_{t-1})\right]. \tag{A9}$$

In Equation (A9), $J \ge 0$ if H_0 holds, while $J < 0$ if H_1 holds. Jeong et al. (2012) show that a feasible kernel-based test statistic for J is as follows:

$$\widehat{J}_T = \frac{1}{T(1-1)h^{2p}} \sum_{t=k+1}^{T} \sum_{s=k+1, s\neq t}^{T} K\left(\frac{W_{t-1} - W_s}{h}\right)\widehat{\varepsilon}_t\widehat{\varepsilon}_s, \tag{A10}$$

where K (·) denotes the kernel function with bandwidth h and T, k, $\widehat{\varepsilon}_t$ are the sample size, the lag-order and estimate of the unknown regression error, respectively. The estimate of the regression error is the following:

$$\widehat{\varepsilon}_t = 1\left\{\Delta tb_t \le Q_\tau\left(TB_{t-1}\right) - \tau\right\}. \tag{A11}$$

We further use the nonparametric kernel method to estimate the τ-th conditional quantile of Δtb_t given TB_{t-1} as $\widehat{Q}_\tau(TB_{t-1}) = \widehat{F}^{-1}_{\Delta tb_t|TB_{t-1}}(\tau|TB_{t-1})$, where $\widehat{F}_{\Delta tb_t|TB_{t-1}}(\Delta tb_t|TB_{t-1})$ is the Nadarya-Watson kernel estimator:

$$\widehat{F}_{\Delta tb_t|TB_{t-1}}(\Delta tb_t|TB_{t-1}) = \frac{\sum_{s\neq t} L\left((TB_{t-1} - TB)/h\right)1(TB_s \le TB_{t-1})}{\sum_{s\neq t} L((TB_{t-1} - TB)/h)} \tag{A12}$$

where with L(·) denotes the kernel function and h is the bandwidth.

Balcilar et al. (2017) extend the framework of Jeong et al. (2012) by developing a test for the second moment, thereby adopting the nonparametric Granger-quantile-causality approach by Nishiyama et al. (2011). With the inclusion of the Jeong et al. (2012) approach, Balcilar et al. (2017) overcome the issue that causality in mean implies causality in variance, thus the hypothesis of quantile Granger causality running from Δq_t to Δtb_t in higher-order moments can be specified as:

$$H_0 = P\left\{F_{\Delta tb_t^K|W_{t-1}}\left\{Q_\tau(TB_{t-1})\middle|W_{t-1}\right\} = \tau\right\} = 1 \; for \; k = 1, 2, \ldots, K, \tag{A13}$$

and

$$H_1 = P\left\{F_{\Delta tb_t^K|W_{t-1}}\left\{Q_\tau(TB_{t-1})\middle|W_{t-1}\right\} = \tau\right\} < 1 \; for \; k = 1, 2, \ldots, K. \tag{A14}$$

Jeong et al. (2012) show that the re-scaled statistics $Th^p\widehat{J}_T/\widehat{\sigma}_0$ is asymptotically normally distributed. To begin with, we test for the nonparametric granger causality in mean (k=1). Failure to reject the null of Granger causality in mean does not imply non-causality in variance. Therefore, we construct the tests for k=2. The last step is to test for causality-in-mean and variance successively. We determine the lag order using SIC of Schwarz (1978). The bandwidth is selected through the use of least squares cross-validation method. We use the Gaussian kernels for K(·) and L(·).

Hacker and Hatemi-J (2012)

Under the conditional of normal distribution, the Wald statistic in Eq. (10) has a $\chi 2$ distribution asymptotically with p degrees of freedom. However, if the sample size is small and the assumption of normality is violated with time-varying volatility, then the asymptotic critical values for the Wald test are not precise. To deal with it, we will apply the bootstrap test with leverage adjustment as suggested by Hacker and Hatemi-J (2012). This test allows for the role of time-varying effects performs also well when the lag order is endogenously selected. In this context, we first computed the sub-sample size (ss) within equation (A15) to implement the time-varying form of the Hacker and Hatemi-J (2012) causality test.

$$ss = \left[T\left(0.01 + 1.8/\sqrt{T}\right)\right] \tag{A15}$$

Equations (6) -(9) and (A15) consider the role of time-varying effects, while we enhanced the empirical analysis by incorporating asymmetry. To this aim, we assess the relationships between q_t and tb_t departing from the linear regression model, defined as $tb_t = \delta_0 + \delta_1 q_t + \psi D_t + \omega_t$. Additionally, we consider the role of asymmetry: Let us assume that q_t is an integrated variable with data generating process $q_t \equiv q_{t-1} + e_{1t} = q_0 + \sum_{i=1}^{T} e_{1i}$, where q_0 is the initial value of q, and $\mathrm{e}_{1\mathrm{i}}$ is i.i.d. with variance $\sigma^2_{e_1}$. In Hatemi-J (2012), positive shocks are defined as $e^+_{1t} = max(e_{1t}, 0)$; while negative shocks are defined as $e^-_{1t} = min(e_{1t}, 0)$. This implies that $e_{1t} = e^+_{1t} + e^-_{1t}$; while $q_t = q_0 + \sum_{i=1}^{t} e^+_{1t} + \sum_{i=1}^{t} e^-_{1t}$. Hatemi-J (2012) defines positive and negative shocks of each variable in a cumulative form as $q^+_t = \sum_{i=1}^{t} e^+_{1t}$ and $q^-_t = \sum_{i=1}^{t} e^-_{1i}$.

Combined Time- and Frequency-Domain Causality Tests

Partial Wavelet Coherence

The wavelet partial spectrum (WPS), denoted $\left[W^x_n\right]^2$, assesses the local variance of each variable. By means of Monte Carlo simulations, Torrence and Compo (1998) show that the distribution of the local WPS can be expressed as:

$$D\left(\frac{\left[W^x_n(s)\right]^2}{\sigma^2_x} < p\right) \rightarrow \frac{1}{2} P_f x^2_v. \tag{16}$$

The Cross-Wavelet Power (CWP) indicates the zone in the time-scale domain where the time series display high mutual power. The CWP captures the local covariance of two time series in each frequency and shows the quantitative similarities between them. This allows us to locate the regions where Δq_t and Δtb_t co-move in the time–frequency space. For each signal Δq and Δtb we specify the individual wavelet spectra as $W^{\Delta q}_n(s)$ and $W^{\Delta tb}_n(s)$. The Cross-Wavelet between two signals is expressed as:

$$CWS_n^{\Delta q \Delta tb}(s) = W_n^{\Delta q}(s) W_n^{\Delta tb^*}(s), \tag{17}$$

where $W_n^{\Delta tb^*}$ is the complex conjugate of $W_n^{\Delta tb}(s)$. The CWP is thus defined as $\left|W_n^{\Delta q \Delta tb}\right|$

The Wavelet Coherence (WC) of two series $\Delta q = \left\{\Delta q_{\mathrm{n}}\right\}$ and $\Delta tb = \left\{\Delta tb_{\mathrm{n}}\right\}$ is the localized correlation coefficient among these variables in the time–frequency domain. We calculate the WC as the squared absolute value of the smoothed CWS normalized by the product of the smoothed individual WPS of each variable:

$$R^2(u,s) = \frac{\left|S\left(s^{-1} W_{\Delta q \Delta tb}(u,s)\right)\right|^2}{S\left(s^{-1}\left|W_{\Delta q}(u,s)\right|^2\right) S\left(s^{-1}\left|W_{\Delta tb}(u,s)\right|^2\right)} \tag{18}$$

Wavelet Quantile Correlation

Following Li et al. (2015), $Q_{\tau,\Delta q}$ is the τ-th quantile of Δq, and $Q_{\tau,\Delta tb}(\Delta q)$ the τ-th quantile of Δtb conditioning on Δq. Δq is assumed to be independent of Δtb. The quantile covariance can be explained as:

$$Qcov_t(\Delta tb, \Delta q) = cov\{I(\Delta tb - Q_{\tau,Y} > 0, \Delta q)\} = E(\varphi_\tau\left(\Delta tb - Q_{\tau,Y}\right)(\Delta q - E(Y)), \tag{19}$$

where $0 < \tau < 1$ and $\varphi_\tau(w) = \tau - I(w < 0)$. Following Li et al. (2015 we calculate the quantile correlation as:

$$QC_t(\Delta tb, \Delta q) = \frac{cov_t(\Delta tb, \Delta q)}{\sqrt{var(\varphi_\tau(\Delta tb - Q_{\tau,\Delta tb}))var(\Delta q)}} \tag{20}$$

The quantile correlation method is extended by Kumar and Padakandla (2022) by means of a maximal overlapping discrete wavelet transform for decomposing Δq_t and Δtb_t. Pairs of Δq_t and Δtb_t are decomposed at the j_{th} level, and quantile correlation techniques are applied to get the wavelet quantile correlation for each level j. Wavelet quantile correlation is:

$$WQC_t(\Delta tb, \Delta q) = \frac{QC_t(d_j[\Delta tb], d_j[\Delta q])}{\sqrt{var(\theta_\tau(d_j[\Delta tb] - Q_{\tau,d_j[\Delta tb]}))var(d_j[\Delta q])}} \tag{21}$$

In Equation (A21), Δq is the independent series and Δtb the dependent series. By representing the association between Δq and Δtb at different quantiles, wavelet quantile correlation handles the effects of the outliers as shocks and captures the likely asymmetric associations between the model parameters.

Supplementary Information The online version contains supplementary material available at https://doi.org/10.1007/s11079-025-09807-7.

Acknowledgements This work has been carried out thanks to the financial support of the research project PID2022-137648OB-C21, funded by Ministerio de Ciencia e Innovación (Madrid), MCIN/AEI/10.13039/501100011033 and by the European Regional Development Fund, "ERDF A way of making Europe".

Funding Open Access funding provided thanks to the CRUE-CSIC agreement with Springer Nature.

Data Availability The datasets are all publicly available, compiled by Eurostat.

Declarations

Conflict of interest There are no conflicts of interest.

References

Ahmed A, Granberg M, Troster V, Uddin GS (2020) Asymmetric dynamics between uncertainty and unemployment flows in the United States. Stud Nonlinear Dyn Econom. https://doi.org/10.1515/SNDE-2019-0058

Ahmed A, Granberg M, Troster V, Uddin GS (2022) Asymmetric dynamics between uncertainty and unemployment flows in the United States. Stud Nonlinear Dyn Econom 26(1):155–172. https://doi.org/10.1515/SNDE-2019-0058/

Allsop C, Vines D (2010) Fiscal Policy, intercountry adjustment and the real exchange rate within Europe. In: Buti M et al. (Ed.) The Euro: The First Decade. Cambridge University Press. https://ideas.repec.org/p/euf/ecopap/0344.html

Bahmani M, Harvey H, Hegerty SW (2013) Empirical tests of the Marshall-Lerner condition: A literature review. J Econ Stud 40(3):411–443. https://doi.org/10.1108/01443581311283989

Bahmani-Oskooee M, Fariditavana H (2016) Nonlinear ARDL approach and the J-curve phenomenon. Open Econ Rev 27(1):51–70. https://doi.org/10.1007/S11079-015-9369-5/TABLES/6

Bahmani-Oskooee M, Karamelikli H (2021a) Asymmetric J-curve: evidence from UK-German commodity trade. Empirica 48(4):1029–1081. https://doi.org/10.1007/S10663-021-09502-Z/TABLES/7

Bahmani-Oskooee M, Karamelikli H (2021b) Estimating a bilateral J-curve between the UK and the Euro area: An asymmetric analysis. Manch Sch 89(2):223–237. https://doi.org/10.1111/MANC.12358

Bahmani-Oskooee M, Nouira R (2021a) U.S.-German commodity trade and the J-curve: New evidence from asymmetry analysis. Econ Syst 45(2):100779. https://doi.org/10.1016/J.ECOSYS.2020.100779

Bahmani-Oskooee M, Nouira R (2021b) U.S. – Italy commodity trade and the J-curve: new evidence from asymmetry analysis. Int Econ Econ Policy 18(1):73–103. https://doi.org/10.1007/S10368-020-00472-4/FIGURES/1

Bajo-Rubio O, Berke B, Esteve V (2016) The effects of competitiveness on trade balance: The case of southern europe. Economics 10(1):1–26

Balcilar M, Bekiros S, Gupta R (2017) The role of news-based uncertainty indices in predicting oil markets: a hybrid nonparametric quantile causality method. Empir Econ 53(3):879–889. https://doi.org/10.1007/S00181-016-1150-0/FIGURES/2

Belke A, Dreger C (2013) Current account imbalances in the euro area: does catching up explain the development? Rev Int Econ 21(1):6–17. https://doi.org/10.1111/ROIE.12016

Bilbao-Ubillos J, Fernández-Sainz A (2019) A critical approach to wage devaluation: The case of Spanish economic recovery. Soc Sci J 56(1):88–93. https://doi.org/10.1016/J.SOSCIJ.2018.05.006

Bilbao-Ubillos J, Fernández-Sainz A-I (2022) The results of internal devaluation policy as a crisis exit strategy: The case of Spain. Global Pol. https://doi.org/10.1111/1758-5899.13120

Brock WA, Scheinkman JA, Dechert WD, LeBaron B (1996) A test for independence based on the correlation dimension. Economet Rev 15(3):197–235. https://doi.org/10.1080/07474939608800353

El-Shagi M, Lindner A, von Schweinitz G (2016) Real Effective Exchange Rate Misalignment in the Euro Area: A Counterfactual Analysis. Rev Int Econ 24(1):37–66. https://doi.org/10.1111/ROIE.12207

Engle RF, Manganelli S (2012) CAViaR. J Bus Econ Stat 22(4):367–381. https://doi.org/10.1198/073500104000000370

European Commission (2011) Quarterly report on the euro area. Office for Official Publications of the European Communities

Fukui M, Nakamura E, Steinsson J (2023) The macroeconomic consequences of exchange rate depreciations (No. w31279). National Bureau of Economic Research

Goldstein M, Khan MS (1985) Income and price effects in foreign trade. Handb Int Econ 2(C):1041–1105. https://doi.org/10.1016/S1573-4404(85)02011-1

Granger CWJ (1969) Investigating causal relations by econometric models and cross-spectral methods. Econometrica 37(3):424. https://doi.org/10.2307/1912791

Hacker S, Hatemi-J A (2012) A bootstrap test for causality with endogenous lag length choice: Theory and application in finance. J Econ Stud 39(2):144–160. https://doi.org/10.1108/01443581211222635/FULL/PDF

Hamilton JD (1994) Time series analysis. Princeton University Press, Princeton

Hatemi-J A (2012) Asymmetric causality tests with an application. Empir Econ 43(1):447–456. https://doi.org/10.1007/S00181-011-0484-X

Hein E, Meloni WP, Tridico P (2021) Welfare models and demand-led growth regimes before and after the financial and economic crisis. Rev Int Polit Econ 28(5):1196–1223. https://doi.org/10.1080/09692290.2020.1744178

Iqbal J, Nosheen M, RehmanPanezaiSalahuddin G (2021) Asymmetric cointegration, Non-linear ARDL, and the J-curve: A bilateral analysis of Pakistan and its trading partners. Int J Fin Econ 26(2):2263–2278. https://doi.org/10.1002/IJFE.1905

Ivanovski K, Awaworyi Churchill S, Nuhu AS (2020) Modelling the Australian J-Curve: An ARDL cointegration approach. Econ Papers: J Appl Econ Policy 39(2):167–184. https://doi.org/10.1111/1759-3441.12277

Jeong K, Härdle WK, Song S (2012) A consistent nonparametric test for causality in quantile. Economet Theor 28(4):861–887. https://doi.org/10.1017/S0266466611000685

Karamelikli H (2016) Linear and nonlinear dynamics of the Turkish trade balance f the Turkish trade balance. Int J Econ Financ 8(2):70–80. https://doi.org/10.5539/ijef.v8n2p70

Kohler K, Stockhammer E (2022) Growing differently? Financial cycles, austerity, and competitiveness in growth models since the Global Financial Crisis. Rev Int Polit Econ 29(4):1314–1341. https://doi.org/10.1080/09692290.2021.1899035

Krugman P (2012) End this depression now!. W. W. Norton & Company, New York

Krugman P, Taylor L (1978) Contractionary effects of devaluation. J Int Econ 8(3):445–456. https://doi.org/10.1016/0022-1996(78)90007-7

Kumar AS, Padakandla SR (2022) Testing the safe-haven properties of gold and bitcoin in the backdrop of COVID-19: A wavelet quantile correlation approach. Financ Res Lett 47:102707. https://doi.org/10.1016/J.FRL.2022.102707

Kurozumi E, Yamamoto T (2000) Modified lag augmented vector autoregressions. Economet Rev 19(2):207–231. https://doi.org/10.1080/07474930008800468

Li G, Li Y, Tsai CL (2015) Quantile correlations and quantile autoregressive modeling. J Am Stat Assoc 110(509):246–261. https://doi.org/10.1080/01621459.2014.892007

Magee SP (1973) Currency contracts, pass-through, and devaluation. Brook Pap Econ Act 1973(1):325. https://doi.org/10.2307/2534091

Mwito MM, Mkenda BK, Luvanda E (2021) The asymmetric J-curve phenomenon: Kenya versus her trading partners. Central Bank Rev 21(1):25–34. https://doi.org/10.1016/J.CBREV.2020.09.001
Nishiyama Y, Hitomi K, Kawasaki Y, Jeong K (2011) A consistent nonparametric test for nonlinear causality—Specification in time series regression - ScienceDirect. J Econ 165(1):112–127
Nogueira RP, León-Ledesma MA (2011) Does exchange rate pass-through respond to measures of macroeconomic instability? J Appl Econ 14(1):167–180. https://doi.org/10.1016/S1514-0326(11)60010-X
Nusair SA (2016) The J-Curve phenomenon in European transition economies: A nonlinear ARDL approach. 31(1), 1–27. https://doi.org/10.1080/02692171.2016.1214109
Percival D, Walden A (2000) Wavelet methods for time series analysis. Cambridge University Press
Rose AK, Yellen JL (1989) Is there a J-curve? J Monet Econ 24(1):53–68. https://doi.org/10.1016/0304-3932(89)90016-0
Schwarz G (1978) Estimating the dimension of a model. Ann Stat 6(2):461–464. https://doi.org/10.1214/aos/1176344136
Shin Y, Yu B, Greenwood-Nimmo M (2014) Modelling Asymmetric Cointegration and Dynamic Multipliers in a Nonlinear ARDL Framework. In Festschrift in Honor of Peter Schmidt. Springer New York, pp 281–314. https://doi.org/10.1007/978-1-4899-8008-3_9
Torrence C, Compo GP (1998) A practical guide to wavelet analysis. Bull Am Meteor Soc 79(1):61–78. https://doi.org/10.1175/1520-0477(1998)079
Troster V (2018) Testing for granger-causality in quantiles. Econ Rev 37(8):850–866. https://doi.org/10.1080/07474938.2016.1172400
Troster V, Shahbaz M, Uddin GS (2018) Renewable energy, oil prices, and economic activity: a Granger-causality in quantiles analysis. Energy Econ 70:440–452. https://doi.org/10.1016/J.ENECO.2018.01.029
Upadhyaya KP, Mixon FG, Bhandari R (2022) Is there a J-curve in China-U.S. trade? Int J Fin Econ 27(1):61–67. https://doi.org/10.1002/IJFE.2137
Xifré R (2017) Competitividad y comportamiento de las exportaciones: España en el contexto de la eurozona. Cuad Inform Econ 260:27–37 (http://ec.europa.eu/economy_finance/db_indicators/competitiveness/)
Yilanci V, Kilci EN (2021) The role of economic policy uncertainty and geopolitical risk in predicting prices of precious metals: Evidence from a time-varying bootstrap causality test. Resour Policy 72:102039. https://doi.org/10.1016/J.RESOURPOL.2021.102039